Tellus (1983), *35A*, 269–286

Effects of orography on Mediterranean lee cyclogenesis and its relationship to European blocking

By S. TIBALDI, *European Centre for Medium Range Weather Forecasts, Shinfield Park, Reading, Berkshire RG2 9AX, England, and* A. BUZZI, *FISBAT-CNR, c/o Istituto di Fisica 'A.Righi', Via Irnerio 46, Bologna, Italy*

(Manuscript received May 10; in final form October 26, 1982)

ABSTRACT

The rôle of orographically-induced cyclogenesis in the lee of the Alps in favouring the onset of Euro-Atlantic blocking is investigated by means of numerical simulations of a real case. The model used is the ECMWF global grid-point model as operational in August 1980. While the essential part that the local orography (the Alps) plays in triggering the development of cyclonic disturbances is confirmed for the first time using a global model, the relationship between Alpine cyclogenesis and European blocking remains less clear. The importance of global orography in generating and maintaining the blocking pattern is subsequently investigated and its crucial rôle evidenced and discussed.

1. Introduction

During the period of formation of blocking situations over Europe, the Mediterranean is dominated, on average, by an area of relative depression, being affected by troughs or cut-off lows which are the counterpart of the high pressure that establishes itself over the north-eastern Atlantic or over Northern Europe.

In various studies of blocking which have appeared in the literature (e.g. Rex, 1950; Austin, 1980; Hartman and Ghan, 1980) attention has mostly been devoted to the blocking anticyclone that develops and persists at high latitudes, rather than to the whole associated circulation. The reason is probably that the anticyclone has a more defined and persistent character ("centre of action") than the surrounding, more mobile, lows. However, from a dynamical point of view, it is not obvious that the rôle of these lows is secondary in importance for the establishment and maintenance of the blocking equilibrium. Green (1977) pointed out that baroclinic eddies steered around the blocking high, along the two split branches of the westerly jet, are important in maintaining the block through the momentum and vorticity fluxes associated with them. This mechanism seems more relevant to the maintenance rather than to the onset of blocking.

Concerning more specifically the investigation of the possible rôle played by cyclogenesis in the formation of blocking, Illari et al. (1981), hereafter referred to as IMS, recently pointed out that cyclogenesis in the Mediterranean assumes, in some cases, the character of an "absolute" (or "in place") instability, resulting in the formation of stationary or slowly moving cut-off lows. They noted that this process is often associated with the breakdown of the westerlies over the Eastern Atlantic and Western Europe. The interruption of the mid-latitude westerly flow can be short-lived or can, sometimes, lead to a persistent blocking situation in the manner schematically described by Berggren et al. (1949). The typical transition from an absolute cyclogenesis in the Mediterranean to a European blocking strongly resembles a vortex–vortex interaction, with the final, stable, configuration showing a vortex pair with an anomalous high to the north and a low to the south. Ji and Tibaldi (1982) also pointed out the apparent similar need for a deep cyclogenesis off the east coast of North America to trigger off Western Atlantic Blocking.

There is, therefore, some observational evidence of a connection between deep cyclonic formation over the Mediterranean and European blocking. Since a large number of cyclogeneses in the Western and Central Mediterranean are lee cyclogeneses caused or modified by the surrounding topography (Buzzi and Tibaldi, 1978, hereafter referred to as BT), we can also hypothesize an indirect link between the orography of Southern Europe (the Alps in particular) and European blocking. It is this aspect that originally prompted this work.

There are also some *theoretical considerations* that support the idea of a link between the absolute (in the IMS sense) cyclogenesis and blocking. A blocking situation is in general associated with anomalous amplitudes of the first few zonal wavenumber components in the middle troposphere (Austin, 1980; Colucci et al., 1981). However, the anomaly associated with a block is usually confined to a limited geographical area, its shape has repetitive characteristics and its existence is often very stable with respect to upstream and downstream changing conditions. All these characteristics support the concept of a "local" (on the planetary scale) persistent disturbance. This, in other words, means that the atmosphere is in a locally stable state, possibly of the kind suggested by the solutions of McWilliams (1980), free modon, Trevisan and Buzzi (1980), solution with forcing and Malguzzi and Speranza (1981), nonlinear local resonance. In all of these cases the non-linearity plays a fundamental rôle in determining the equilibrium properties of the solution. It therefore seems plausible that local disturbances which tend to establish a flow pattern (splitting of the jet, cut-off lows at middle-low latitudes) resembling that of blocking and in the right position (localized forcing being probably important) can lead to a proper blocking state, considering also that this state could have an "attracting" nature in the phase space of the atmospheric system (Charney and De Vore, 1979).

If the physical problem of how to maintain an atmospheric blocking is still very controversial, even less is known theoretically about the time-dependent problem of the entrance into a blocking situation. In this paper we describe how we tried to gain some insight into this problem by means of numerical experiments on a case of European blocking preceded by a deep cyclogenesis in the lee of the Alps. As more extensively reported below, the synoptic analysis of the event chosen suggests a link between cyclogenesis and blocking, in the sense that the former seemed to have favoured the onset of the latter or, at least, controlled its shape and characteristics. A second aim of this work is to study the behaviour of a model designed for large-scale simulation and prediction, in the presence of a phenomenon like lee cyclogenesis which is initiated by the action of a topographic obstacle (the Alps) whose scale is only marginally resolved by the model grid.

We also report here a preliminary result concerning the rôle of a large-scale orographic forcing in producing and maintaining atmospheric blocking. It is well known (e.g. Rex, 1950) that the frequency of blocks peaks over well-defined geographical areas. This suggests that the location of blocking is directly controlled by fixed atmospheric forcings, or by planetary stationary waves in turn controlled by fixed geographical forcings. Previous studies (e.g. Charney and Eliassen, 1949; Manabe and Terpstra, 1974; Grose and Hoskins, 1979) have shown that mountains are a major source of planetary waves. One of our numerical experiments was designed with the purpose of investigating the rôle played by the global orography.

We choose, for our experiments, the N48 grid-point model in operation at the European Centre for Medium Range Weather Forecasts (ECMWF). It is a global model and includes a rather sophisticated parameterization of physical effects: it is therefore suitable for describing planetary scale dynamics and performing realistic medium range (4 to 10 days) integrations. A satisfactory skill of this model in forecasting blocking has also been reported by Bengtsson (1981), Tibaldi and Ji (1983) and Ji and Tibaldi (1982). The resolution of the ECMWF global model is also high enough (1.875° regular lat/long grid in the horizontal and 15 levels in the vertical) for the effect of the Alps to be described, at least to a simple extent. The reader is also referred to Tibaldi and Buzzi (1982) for a more detailed report on these numerical experiments.

2. The case study

The period of the case study embraces the last week of November and the first week of December 1978. The first 3 weeks of November were characterized by an almost zonal flow over the

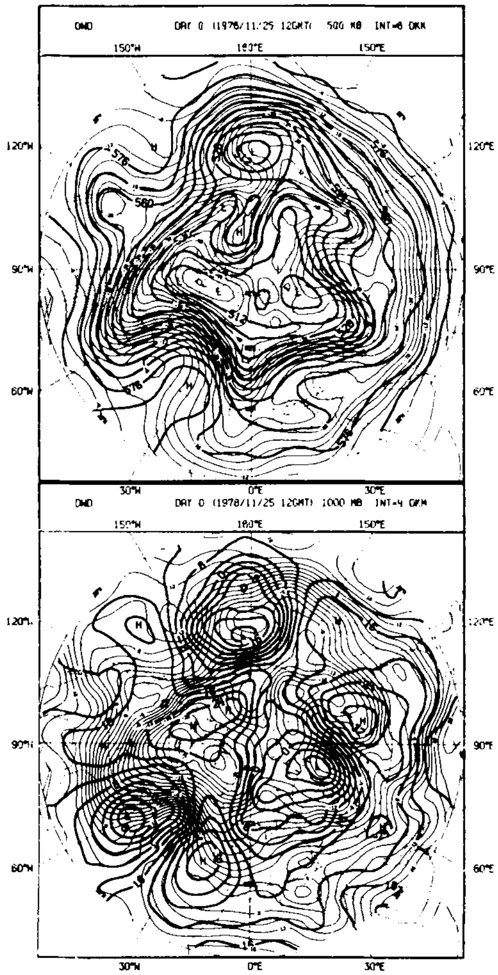

Fig. 1. Deutsche Wetterdienst analyses (top: 500 mb height and temperature, bottom: 1000 mb height and 850 mb temperature) for 12 GMT 25 November 1978. Initial conditions for all numerical experiments (day 0). 500 mb heights drawn every 8 dam, 1000 mb heights every 4 dam. 500 mb and 850 mb temperatures drawn every 2 °C.

Atlantic and Western Europe, with the axis of the westerlies displaced in an anomalously northern position, so that the Mediterranean was dominated by anticyclonic conditions.

Between the 23rd and the 27th, a dramatic change took place in the circulation over the Atlantic and Europe. A large amplitude trough–ridge system rapidly developed at 500 mb over the east coast of North America and the middle Atlantic on the 24th and the 25th, respectively, followed by a deepening of a downstream trough over Europe. The development of this latter trough was accompanied by a lee cyclogenesis that started between the 25th at 12 GMT and the 26th at 00 GMT over the Gulf of Genoa at low levels and evolved during the 28th and the 29th into a deep cyclone (the minimum pressure value being around 985 mb) moving very slowly south-eastwards in the central Mediterranean (see Figs. 1 and 2a–5a). A corresponding cut-off low formed at 500 mb between the 27th and 28th and deepened further in the following 24 hours (see Figs. 3a–5a).

After the 29th at 00 GMT, the Mediterranean cyclone drifted rapidly eastwards while filling, both near the surface and at high levels. It was in this stage, however, that the blocking circulation was set up over Europe. The process is better followed at 500 mb in Figs. 4a–7a: between the 28th at 00 GMT and 29th at 00 GMT, the Atlantic ridge was "squeezed" and moved anticlockwise between the almost stationary Mediterranean vortex and a new trough advancing eastwards in the Western Atlantic, so that an isolated blocking high formed on the 30th at 00 GMT over the Norwegian Sea (figure not shown). At the same time, the westerly jet split over the Atlantic at about 15° west. The blocking circulation then assumed the characteristic omega shape and lasted, with little changes in shape or location, until the 11th.

The evolution of the lee cyclogenesis was consistent, at least in the first 2 days, with the schematic processes outlined in BT. The interaction of the cold front with the Alps produced the initial disturbance which then grew as a baroclinic disturbance. In Fig. 8, two characteristic properties of the lee cyclone, namely intensity and position, are plotted versus time. The cyclone is considered for this purpose as an individual vortex having a scale of about 1000 km. As a measure of its intensity, we took the average pressure difference between the centre of the cyclone and a surrounding circle of 1000 km radius. In order to visualize its propagation and since its movement is mainly from west to east, the longitude of the cyclone centre is also plotted. Fig. 8 shows (for the moment only the graphs marked DWD will be of interest to us) that the initial disturbance (between the 25th at 12 GMT and the 26th at 00 GMT) grew rapidly, that is with an e-folding time of about 10 h, and was followed by a period of slower growth

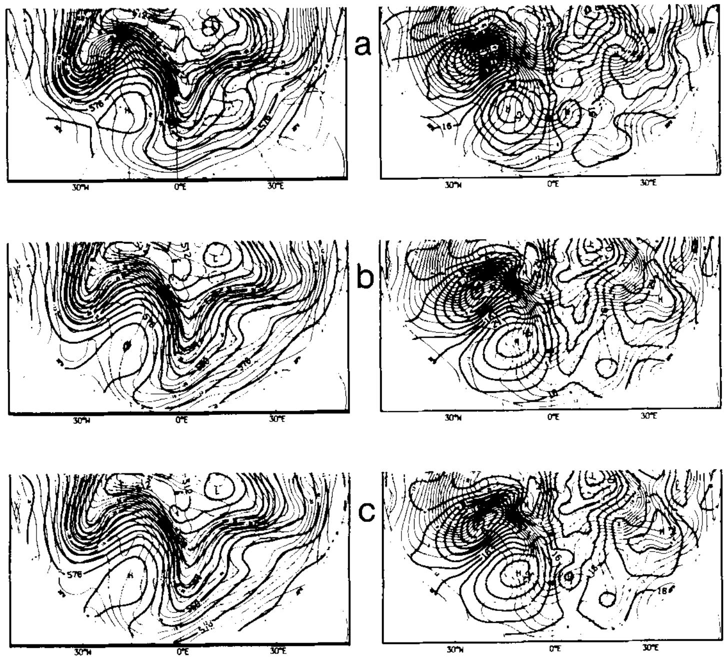

Fig. 2. (a) Same as Fig. 1, but for day 1 (12 GMT 26 November 1978). (b) Same as (a), but for model run D46 (control). (c) Same as (a) but for model run E21 (enhanced Alps).

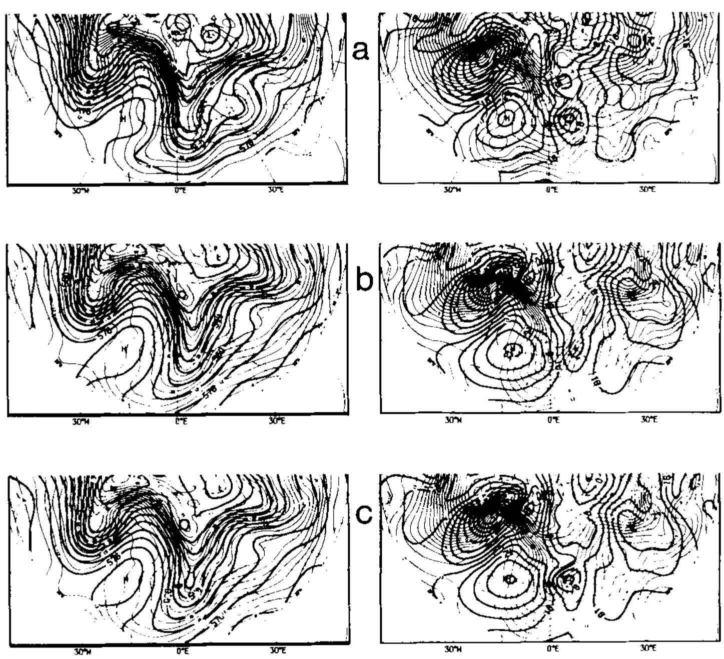

Fig. 3. Same as Fig. 2, but for day $1\frac{1}{2}$ (00 GMT 27 November 1978).

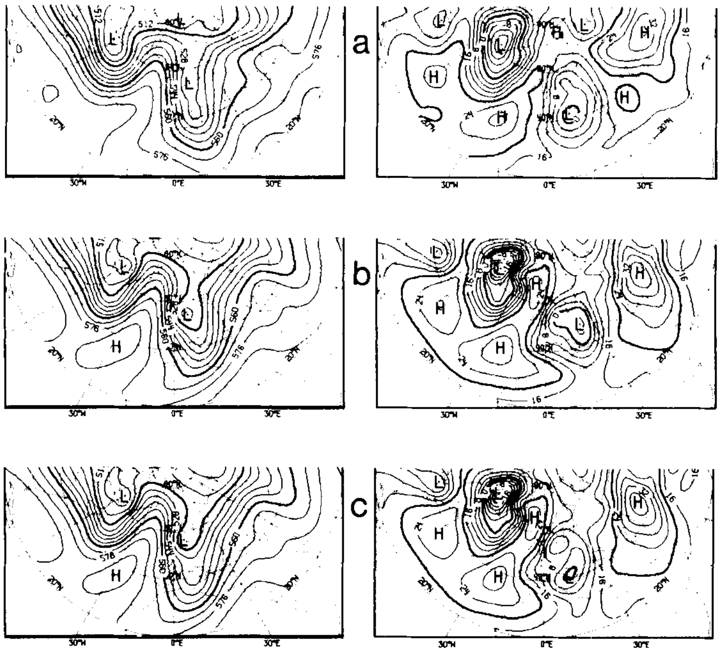

Fig. 4. Same as Fig. 2, but for day 2½ (00 GMT 28 November 1978). Only heights are shown.

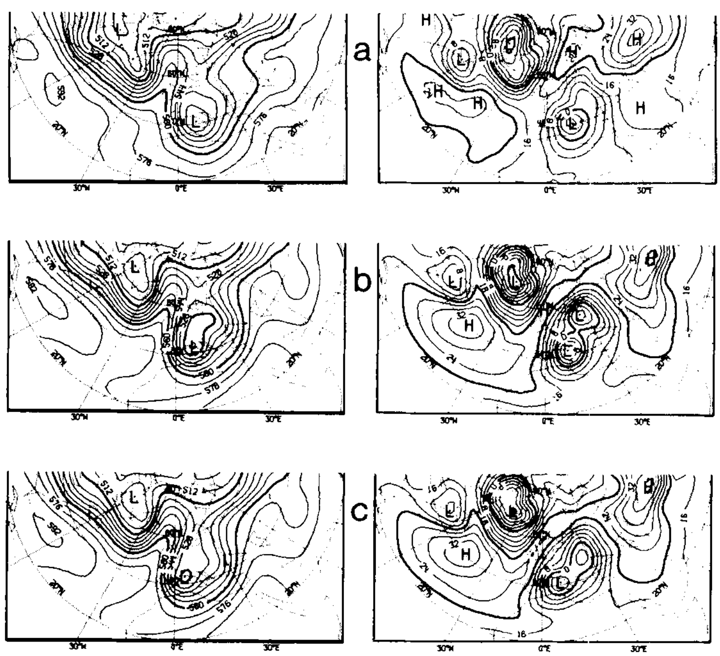

Fig. 5. Same as Fig. 4, but for day 3½ (00 GMT 29 November 1978).

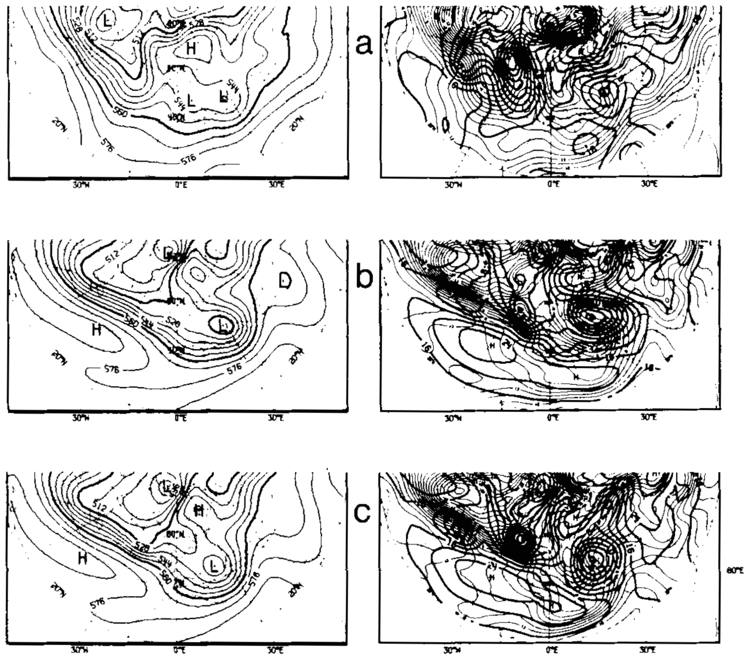

Fig. 6. Same as Fig. 4, but for day 5½ (00 GMT 1 December 1978). 850 mb temperatures are shown again, overlapped with 1000 mb height maps (as for Fig. 1).

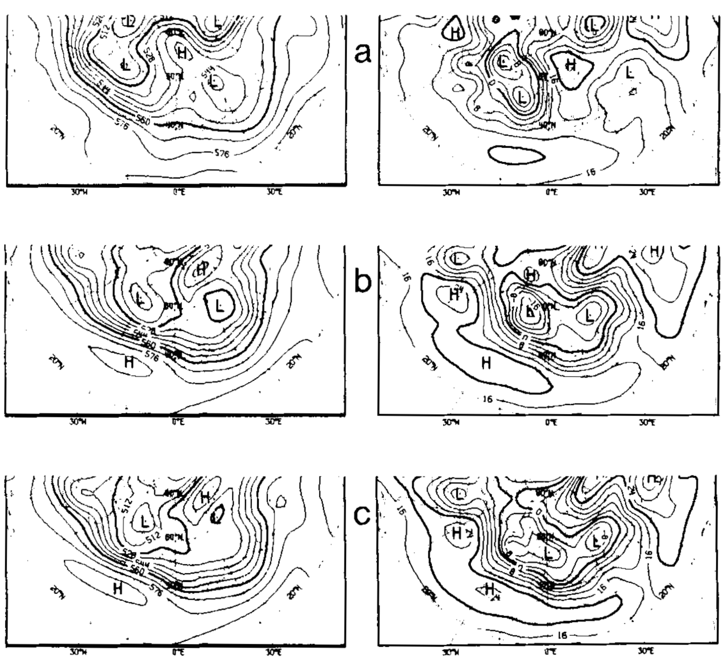

Fig. 7. Same as Fig. 4, but for day 7½ (00 GMT 3 December 1978).

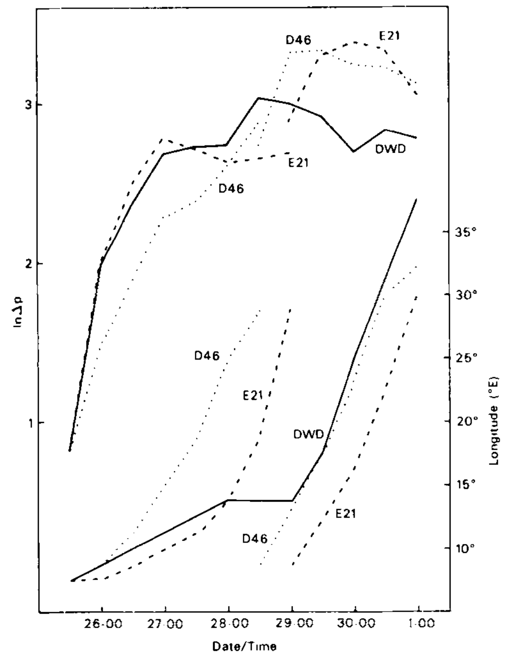

Fig. 8. Intensity of the pressure perturbation (upper set of graphs) associated with the cyclone centre in the lee of the Alps and longitudinal position of the cyclone centre (lower set of graphs) as functions of time (see also text).

(e-folding time of about 30 h). After a period of very little development, from the 27th 00 GMT to the 28th 00 GMT, a new growth phase can be identified during the following 24 h. After the 29th at 00 GMT, the intensity of the surface cyclone started to decline.

With regard to the displacement of the system during its life cycle, we observe that it grew almost in the same place both at the surface and at 500 mb, and only during the decay stage (after 29-00 GMT) drifted considerably eastwards. Following IMS, this cyclogenesis can therefore be classified as absolute. IMS give a criterion, based on the stability theory of barotropic Rossby waves, that allows us to discriminate between absolute and convective instability. The criterion is based on the evaluation of the two parameters:

$$M = Uk^2/\beta \quad \text{and} \quad N = uk^2/\beta,$$

where U and k are the horizontal phase velocity and wave number of the basic state Rossby wave, respectively; u is the basic state zonal wind and β is the local variation of the Coriolis parameter.

IMS theory thus predicts absolute instability, as opposed to convective, when the ratio M/N is larger than a critical value which depends on N itself and on the meridional wavelength of the Rossby wave. Although the validity of the theory is formally restricted to barotropic instability, the analysis of cases of cyclogenesis in the Mediterranean in terms of M and N, represented in Fig. 7 of IMS, reveals that the two regions of convective and absolute instability are well separated in the M, N plane. We have evaluated M and N for our case study, calculating these parameters as described in IMS, at 25-00 GMT, that is before the initiation of the lee cyclogenesis. The values we obtained are $M = 2.5$ and $N = 2.2$, which places this case well into the region of absolute instability. The value of M is even higher if computed on the 25th at 12 GMT, that is just before the appearance of the lee cyclone. In conclusion, this case study was chosen for the following reasons:

(i) a typical cyclogenesis occurred in the lee of the Alps;

(ii) this cyclogenesis was intense, "absolute" in character and extended its influence to the whole of Southern Europe throughout the troposphere;

(iii) its preceded the onset of a blocking circulation over Europe, and the synoptic analysis suggests the hypothesis, to be verified, that the Mediterranean lee cyclogenesis played an important rôle in controlling or modifying the process of blocking formation.

3. The model

The model used is the ECMWF global N48 grid-point model as in operation in August 1980. The model uses the primitive equations on a global regular latitude–longitude grid of 1.875 × 1.875°; it has 48 grid intervals between the poles and the equator (hence the acronym N48) and 192 grid intervals along each line of latitude. The vertical coordinate is the well-known sigma (p/p_{surf}) coordinate (Phillips, 1957). The vertical resolution is of 15 temperature and wind carrying levels, the uppermost being around 25 mb and the lowermost approximately $p_{surf}/20$ mb above the models orography. The (at the time) ECMWF operational model orography was a substantially smoothed version (originally produced at GFDL) of Berkofsky and Bertoni (1955) orography. The finite difference scheme is based on the staggered "C" grid, following Arakawa (Arakawa and Lamb, 1977). This grid was chosen mainly because of its low computational noise and the ease of implementation of a semi-implicit time scheme. Following the work of Arakawa (1966) and Sadourny (1975), the finite difference scheme was designed to conserve potential enstrophy during vorticity advection by the horizontal flow (the primitive equations being written in flux form). For more details on the adiabatic part of the model see Burridge and Haseler (1977) and Burridge (1979).

The parameterization of physical effects (the model's "physics") includes a full hydrological cycle, a relatively detailed stability-dependent representation of boundary and free-atmospheric turbulent fluxes, and an interaction between the computed radiation field and model-generated clouds (Tiedtke et al., 1979). For more general information on the performance of the ECMWF model the reader is referred to Hollingsworth et al. (1980).

4. Description of the experiments and synoptic evaluations

Three significant experiments, consisting of 10 days of integration each, were executed starting with the same initial condition and changing only the orography. In addition, two shorter experiments were run first, in order to choose the optimal initial condition and to test the sensitivity of the integration with respect to it. The first experiment (D46) can be considered as the "control" experiment, and consisted in simply running the operational version (at August 1980) of the ECMWF grid-point model. In the second experiment (E21), the height of the Alps was considerably increased, in order to model the development of the lee cyclone which was missed in D46, and to test the rôle of this development in the subsequent blocking formation. The third experiment (D59) was run with no orography everywhere, as a first attempt to evaluate the impact of the planetary orography on the onset and maintenance of the blocking. This last approach was followed-up further by the work of Ji and Tibaldi (1982).

ECMWF analyses being unavailable for the period of interest, the US National Meteorological Center (NMC) global analyses were used as initial conditions. The mass, wind and moisture data were interpolated from standard pressure levels to the model's sigma surfaces, and then subjected to the ECMWF non-linear normal mode initialization (Temperton and Williamson, 1981; Williamson and Temperton, 1981) before starting the model integrations.

Since the cyclogenetic process started between the 25th at 12 GMT and the 26th at 00 GMT, the initial condition had to be chosen not after the 25th at 12 GMT but, obviously, not too early in view of the aim of simulating the subsequent blocking process. Three preliminary runs of 3 days each, starting from the NMC analyses of 24-12 GMT, 25-00 GMT and 25-12 GMT, showed that the integrations were similar to each other in the region of interest and therefore were comparatively stable with respect to changes in the initial condition. However the existence of substantial discrepancies between the NMC and DWD (Deutscher Wetterdienst) surface analyses at 25-00 GMT over the Western Mediterranean (probably in favour of DWD) suggested the choice of the latest time (25-12 GMT) as the initial condition for the 10-day runs.

4.1 *The control experiment: D46*

As mentioned in Section 3, the orography used in this experiment is very smooth. Fig. 9a shows this orography in the European area. It is immediately evident that the blocking effect of the Alps on the North Westerly cold outbreaks, which, as pointed out in BT, seems an essential mechanism for initiating cyclogenesis, cannot be effective with this model orography.

The evolution of Exp. D46 is illustrated in Figs. 2b–7b. The maps are directly verifiable comparing them with the corresponding DWD analyses just above them. At 26-12 GMT and 27-00 GMT, the failure of D46 in simulating the cyclogenesis in the lee of the Alps and the associated thermal field deformation, including the cold air blocking by the Alps, is becoming apparent from the surface maps (Figs. 2 and 3); even at 500 mb over Europe, there are now significant differences. In particular, the jet splitting over France and UK, which is associated with the subsequent cut-off process over the Mediterranean, is not well simulated.

At 28-00 GMT (Fig. 4), the forecast over the whole of Southern and Eastern Europe is affected by the misrepresentation of the cyclogenetic

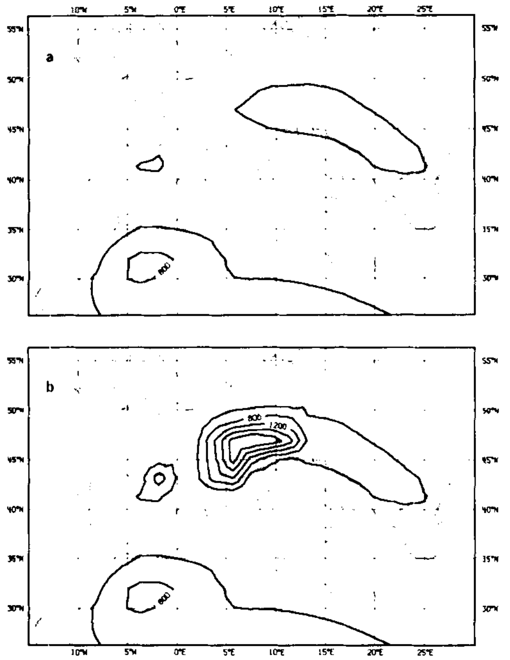

Fig. 9. (a) ECMWF operational orography as at August 1980, in the European area. This orography was used in the control experiment D46. (b) Orography used in experiment E21, in the European area. Contours drawn every 400 m.

process in the Mediterranean. While in the analysis the cyclone is centred over Italy at the surface and a deep trough is present at 500 mb over the Western Mediterranean, in D46 the cyclone, which has formed in the previous 24 h over central Europe and Yugoslavia, is much shifted eastward. Also the southern portion of the European trough at 500 mb is to the east of its real position and too weak. In order to better evaluate the subsequent evolution of the experiment, it is important to note that a second disturbance, characterized by a cold front and a nucleus of cyclonic vorticity advection aloft along the west side of the European trough, grows later and, at 29-00 GMT, leads to a second cyclogenesis over the Western Mediterranean, not due to the presence of the Alps, as shown in Fig. 5b. In Fig. 8, the intensity and longitudinal position of this new cyclone is reported in place of those of the old cyclone for D46 starting from 29-00 GMT. In the real development, only a trace of a second disturbance can be recognized, which reinforces the existing cyclone in the Mediterranean between 28-00 GMT and 28-12 GMT, without substantially changing its location (see Figs. 4a and 5a). The result is that, at 29-00 GMT, the local forecast of D46 over the Mediterranean appears closer to verification than in the previous 2 days due to this spurious development. At 500 mb, the ridging process over the Eastern Atlantic and the cut-off over the Mediterranean are satisfactorily simulated.

A major deficiency of the simulation appears, on the other hand, over the Pacific and North America, where the ridge-trough system in that region is overestimated. This failure appears to affect the subsequent downstream configuration and also the blocking formation over Europe. The forecast at days 5½ and 7½ are reported in Figs. 6 and 7 and show the evolution of the forecast during the second pentad. The blocking configuration on December 1st at 00 GMT is satisfactorily represented by D46 in the large-scale features, although the details are not captured, see Fig. 6b. At 3-00 GMT (Fig. 7b) the forecast has largely deteriorated, though a blocking feature is still present in the model run in a more easterly position than in reality. The run was continued until 5-12 GMT (see Figs. 10a and 10b) when the blocking ridge, still present over Europe in the verification, has weakened substantially in D46 and drifted eastwards, around 40°–50° east.

4.2. *The enhanced Alps experiment: E21*

The second experiment (E21) differs from D46 only in that the local topography in the region of the Alps was arbitrarily modified. The new topography in the region is shown in Fig. 9b. It can be seen that the Alps are much enhanced in height with respect to the "operational" topography, now reaching a maximum of about 2400 m above msl; also the Pyrenees are made slightly higher. This artificial modification of the topography can be questioned, mainly for two reasons: (a) it is not the product of any objective operation on the real topography; (b) the dynamical and physical response of the model to such a steep obstacle of a horizontal scale near the margin of resolution is not obvious and can be subject to shortcomings. However, these new model Alps have been created with the main purpose of having an effective barrier, with maximum height closer to the average height of the "shadow" of the Alpine chain as would be projected on a vertical plane (which

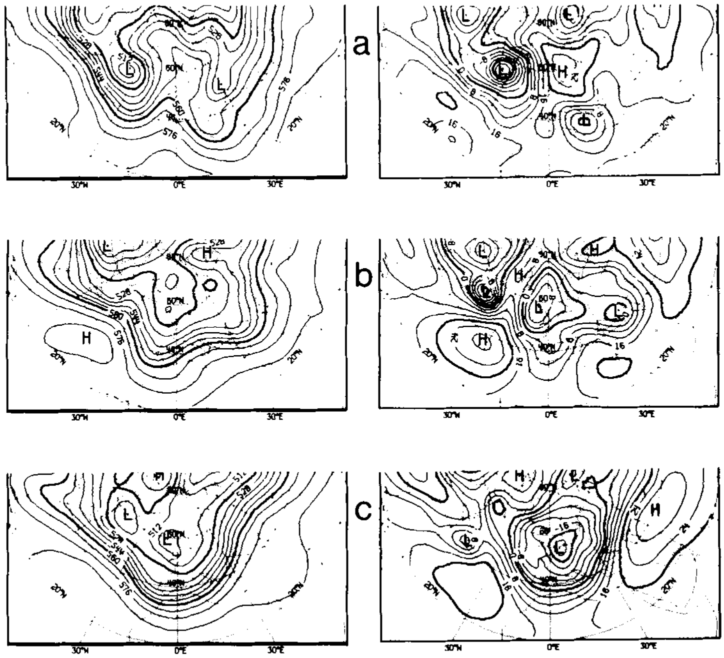

Fig. 10. (a) Same as Fig. 1, but for day 10 (12 GMT 5 December 1978). (b) Same as (a) but for model run D46 (control). (c) Same as (a) but for model run D59 (no mountains). Only geopotential heights are shown.

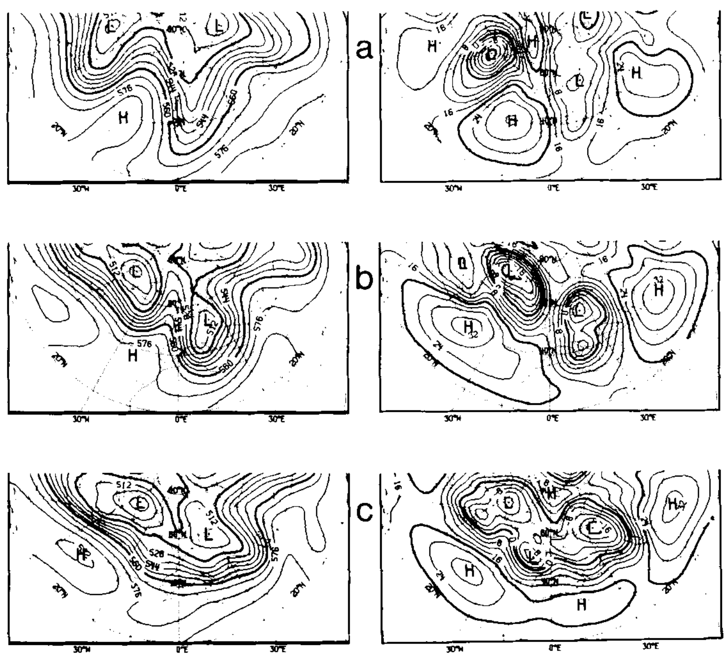

Fig. 11. (a) Same as Fig. 1, but for day $1\frac{1}{2}$ of model run D59 (no mountains). (b) Same as Fig. 1, but for day $3\frac{1}{2}$ of model run D59 (no mountains). (c). Same as Fig. 1, but for day $5\frac{1}{2}$ of model run D59 (no mountains). Only geopotential heights are shown.

exceeds over 3000 m over a large fraction of the chain length). Previous numerical experiments (Bleck, 1977; Tibaldi, 1980; Tibaldi et al., 1980) showed that the lee cyclogenesis phenomenon could be simulated in a rather realistic way, provided that the model Alps had height and steepness comparable to those prescribed here.

The maps resulting from experiment E21 are shown in Figs. 2c–7c. We can see that the cyclogenesis in the lee of the Alps, which was virtually absent in D46, is now reproduced. On the 26th at 12 GMT, the frontal movement over the Alpine region is retarded. The phase of most rapid growth related to this frontal deformation, is very well simulated, as shown in Fig. 2c. The minimum pressure value, its position and the temperature field at 850 mb, showing the cold air penetration over the Western Mediterranean and its blocking over the region south-east of the Alps, are predicted with very good accuracy (Figs. 2 and 3). Even at 500 mb, the forecast is more realistic than in D46: the trough axis over the Western Mediterranean is more to the west than in D46 and the cut-off process has already started.

At 28-00 GMT (Fig. 4c), the E21 forecast is still definitely better than the D46 forecast over the region of interest, but later on, at 29-00 GMT, the 2 experiments tend to become more similar to each other, both showing 2 distinct cyclonic centres at the surface over Europe, while in the analysis, only the cyclone over Italy (with a trough extending north-east of it) is present. The subjective evaluation still indicates that E21 is closer to the analysis than D46, and that the differences between the 2 experiments have spread over a larger region than before, affecting the whole European sector (see also next section). In particular, the cyclone which is over North-eastern Europe in D46, is much weaker in E21 and is in a different position. In the same way, the strong cyclone that is present in D46 over Italy and is the result, as seen previously, of a separate cyclogenetic process, is weaker in E21. This seems to confirm the hypothesis (see Tibaldi et al., 1980) that an isolated obstacle like the Alps tends, in general, to hinder the larger-scale baroclinic development, in spite of the fact that, in special circumstances, they can cause secondary lee cyclogenesis.

The intercomparison of D46 and E21 on December 1, at 00 GMT, i.e. during the stages of formation of blocking (Fig. 6), can give information about the rôle of the Alps and the induced cyclogenesis on the blocking itself. Two things have to be remembered before commenting on the results. First, the blocking is a large-scale phenomenon in nature, and is influenced by many factors (Bengtsson, 1981); therefore all the shortcomings affecting experiment D46, except for the presence of the Alps, also affect experiment E21. Second, the spurious cyclogenesis occurring over the Western Mediterranean at 29-00 GMT in D46 (see Fig. 5) and, to a lesser extent, also in E21, can shield the effects of the previous lee cyclogenesis observed in the verification. Actually, both experiments at 1-00 GMT (see Fig. 6) show to some extent a stronger cyclonic circulation over Eastern Europe than observed, as a consequence of the spurious cyclogenesis. Nevertheless, the differences in the European sector between the 2 experiments are still in favour of E21; they are: (a) the smaller intensity in E21, and the more accurate position (at the surface) of the cyclonic centre over South-eastern Europe; (b) the more pronounced ridge over Spain and Western Europe that stretches towards the high-latitude blocking anticyclone; (c) the temperature field at 850 mb that in E21 protrudes from Scandinavia towards Italy, while in D46 is shifted too much towards the Eastern Mediterranean.

The maps at 3-00 GMT (see Fig. 7) are too far from the initial condition ($7\frac{1}{2}$ days of integration) to derive any firm conclusions from the intercomparison between the 2 experiments. The significant differences observed all over the northern hemisphere are probably not to be interpreted only as dynamically-induced Rossby modes excited by the Alps but also as the result both of propagation of gravity-inertia waves moving away from the Alps and of the growth, due to the natural instability of the model atmosphere, of very small changes introduced everywhere by the non-linear normal mode initialization procedure in response to the local change of the topography. This therefore indicates that, at least in this single experiment, the growth of small errors in the analysis tends to obscure the results after about 1 week of integration.

4.3. *The no mountains experiment: D59*

There is a general consensus in the literature on the importance of the Earth's orography in controlling the phase and intensity of the long stationary waves. The exact mechanisms by which this is

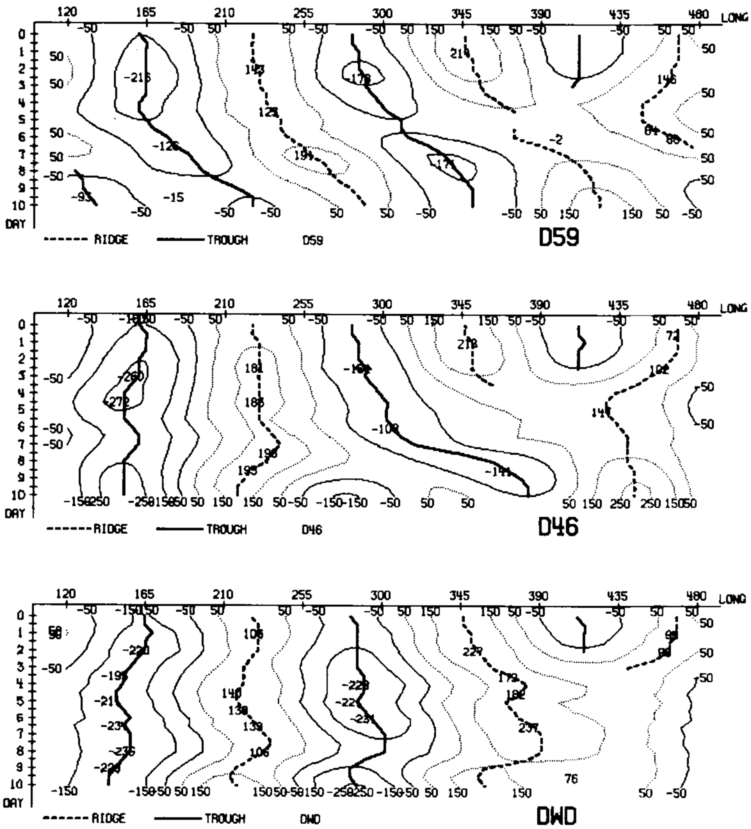

Fig. 12. Hovmöller diagrams for latitude band 35–55° N for wavenumber 1 to 3 waveband—isolines of 500 mb geopotential height as a function of time and longitude. DWD: verifying analysis. D46: control run. D59: no mountains run. Thick continuous lines show the evolution of troughs while thick dashed lines indicate ridges.

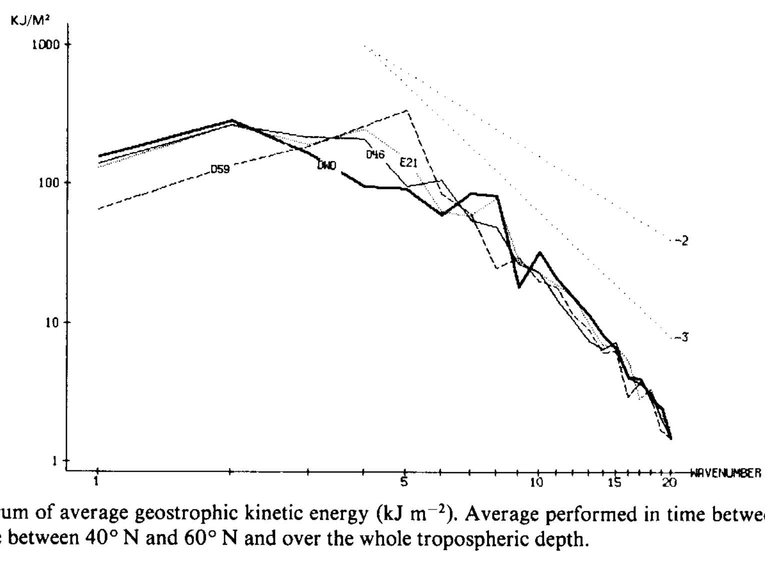

Fig. 13. Spectrum of average geostrophic kinetic energy (kJ m^{-2}). Average performed in time between day 5 and day 10 and in space between 40° N and 60° N and over the whole tropospheric depth.

accomplished have not yet been fully clarified and have been the object of recent investigations (e.g., Charney and Straus, 1980). It is very likely, in any case, that stationary waves and blocking cannot be properly modelled, in intensity and location, if the orographic forcing is neglected. This hypothesis is supported by the outcome of experiment D59, which consists of a 10-day run differing from the previous two only in that the Earth surface was flattened everywhere (the land-sea physical differences were however, maintained). The evolution of experiment D59 is shown in Figs. 11a–c (days 2, 4 and 6), and day 10 is shown in Fig. 10c, where it can be compared directly with D46 and with the verifying analysis.

At 27-00 GMT (Fig. 11a) the forecast does not differ much from E21 and D46, except in regions of extensive mountain complexes, like, for instance, the Himalayas. However, the cyclogenesis in the lee of the Alps is completely missing. At 29-00 GMT (Fig. 11b) the large-scale forecast still preserves some realistic features, particularly in the European sector, where the trough-ridge system, that developed later in the verification into the blocking pattern, is, at this time, apparently predicted not substantially worse than in E21. Nonetheless, over the large continental areas (Asia and North America) the forecast is rapidly deteriorating. This deterioration soon affects the blocking formation over Europe. In fact between 29-00 GMT and 1-00 GMT the Atlantic ridge gradually disappears. As a consequence, a zonal flow re-establishes itself over the Atlantic and Europe, with superimposed short disturbances travelling eastwards (see Fig. 11c). Fig. 12 shows Hovmöller diagrams for the wavenumber band 1 to 3 for the control experiment D46, the no-mountain experiment D59 and for the verifying analyses. It can clearly be seen from these diagrams that the quasi-stationary troughs and ridges well identifiable almost all around the globe (165° E, 230° E, 230° E 345° E) are correctly treated as almost stationary by the control run (with the only exception of the trough at 280° E). The no-mountain run, on the other hand, tends to treat the ultra-long modes as eastward-propagating, because of the absence of the stationary forcing represented by the orography. This effect is particularly evident from day 4 onwards.

Fig. 13 shows the spectrum of kinetic energy for the troposphere, averaged over the last 5 days of integration. It is evident how D46 and E21 behave similarly to each other and to the verification (at least in the overall spectral distribution), with D59 showing an altogether different signature, with much less energy in the ultra-long waves and a spurious peak in wavenumber 5. The effect of the lack of large-scale orographic forcing is again evident.

It is interesting to note that not all of the Northern Hemisphere flow becomes zonal as a consequence of the elimination of the topography. A sort of blocking ridge appears near the west coast of North America in the first few days of integration of D59 (not shown), developing from a ridge present in the initial analysis. This fact could be tentatively taken as an indication that the orographic forcing is not essential to the production of all kinds of blocking patterns, thermal forcing or the formation of a modon-type structure (McWilliams, 1980) being other possible explanations for these phenomena.

5. Some considerations on the rôle of orography

The numerical experiments indicate that the forecast of both lee cyclogenesis in the Mediterranean and European blocking is critically dependent upon the orographic forcing included in the model. The importance of a comparatively small-scale orographic feature like the Alps in modelling this sort of weather development is clearly shown in Fig. 14, where the 1000 mb height 5-day mean maps for the first half of the integrations are shown. While experiment E21 is the only simulation that gives a satisfactory synoptic picture of the circulation over Europe (Fig. 14c), the control run D46 essentially behaves, in this region, like the no-mountain run D59 (Figs. 14b and 14d respectively). This also shows that the effect of a "sudden disappearance" of the large-scale orographic forcing (this is, in fact, what D59 experiment ultimately means) needs a few days to have impact on the model circulation of the global atmosphere.

The importance of the large-scale orography in determining the onset and the conditions for maintenance of the block, and of the large-scale circulation in general, is clearly summarized in Fig. 15, which shows the 500 mb 5-day mean height maps from day 5 to day 10 of the integrations. Experiments D46 and E21 behave similarly during

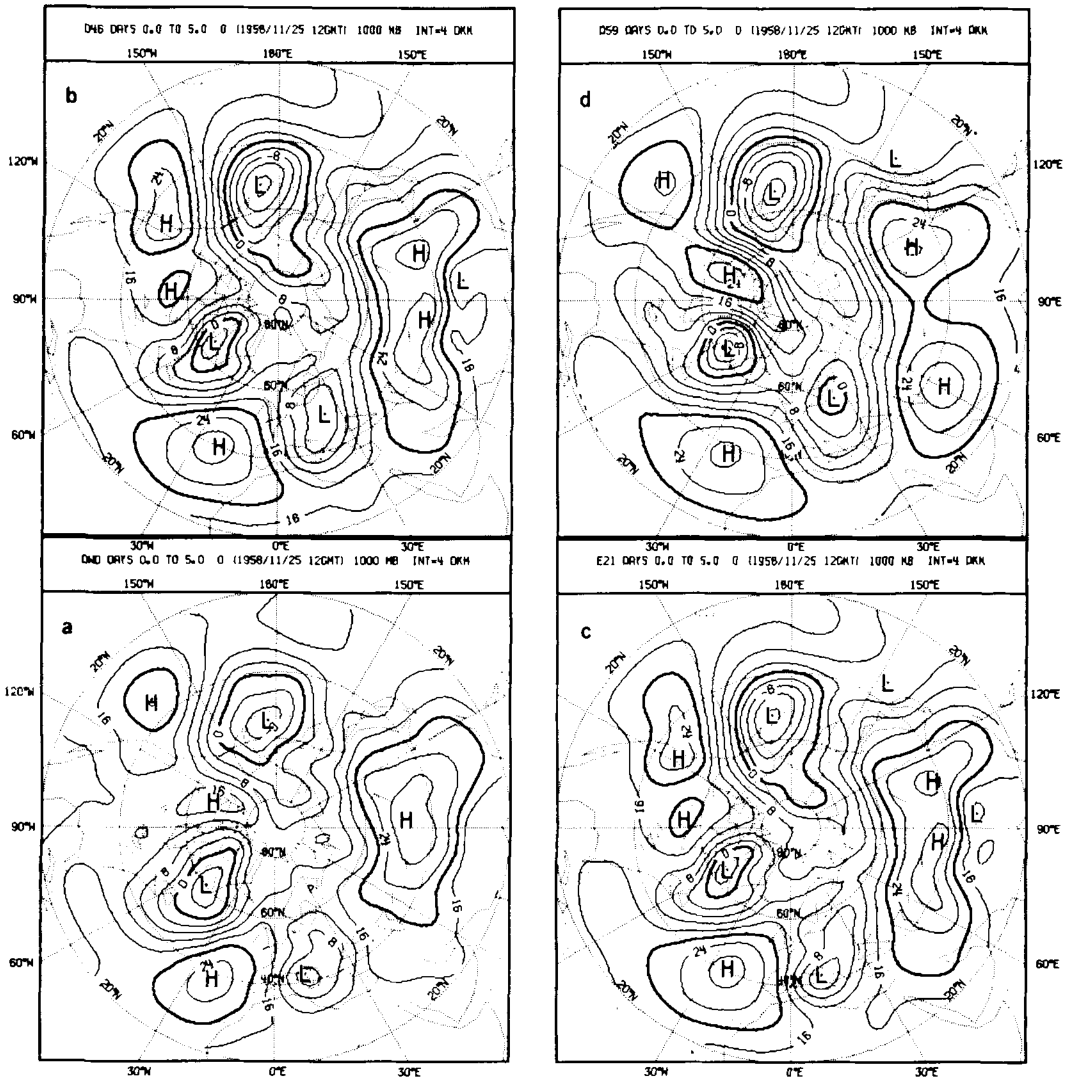

Fig. 14. (a) 1000 mb geopotential height observed 5-day mean map day 0 to 5. (b) as (a) but for experiment D46 (control). (c) as (a) but for experiment E21 (enhanced Alps). (d) as (a) but for experiment D59 (no mountains). Contours are drawn every 4 dam.

this second half of the integration period, producing a block structure over Eastern Europe, that the 5-day mean maps show to be underestimated and displaced in emphasis towards the east. The southerly branch of the split-jet is, accordingly, wrongly emphasized with respect to the northerly portion, in reality much stronger. The positions of the other main troughs in the northern hemisphere are predicted satisfactorily, with the exception of the ridge–trough system over the Rockies and the North American continent which is forecasted 20° to 30° too far to the east of the observed position. D59, conversely, shows no signs of blocking doublet, replacing it with a huge, double-structured, trough that occupies the whole quadrant 30° W–60° E.

Turning our attention to the comparatively smaller differences between experiments D46 and

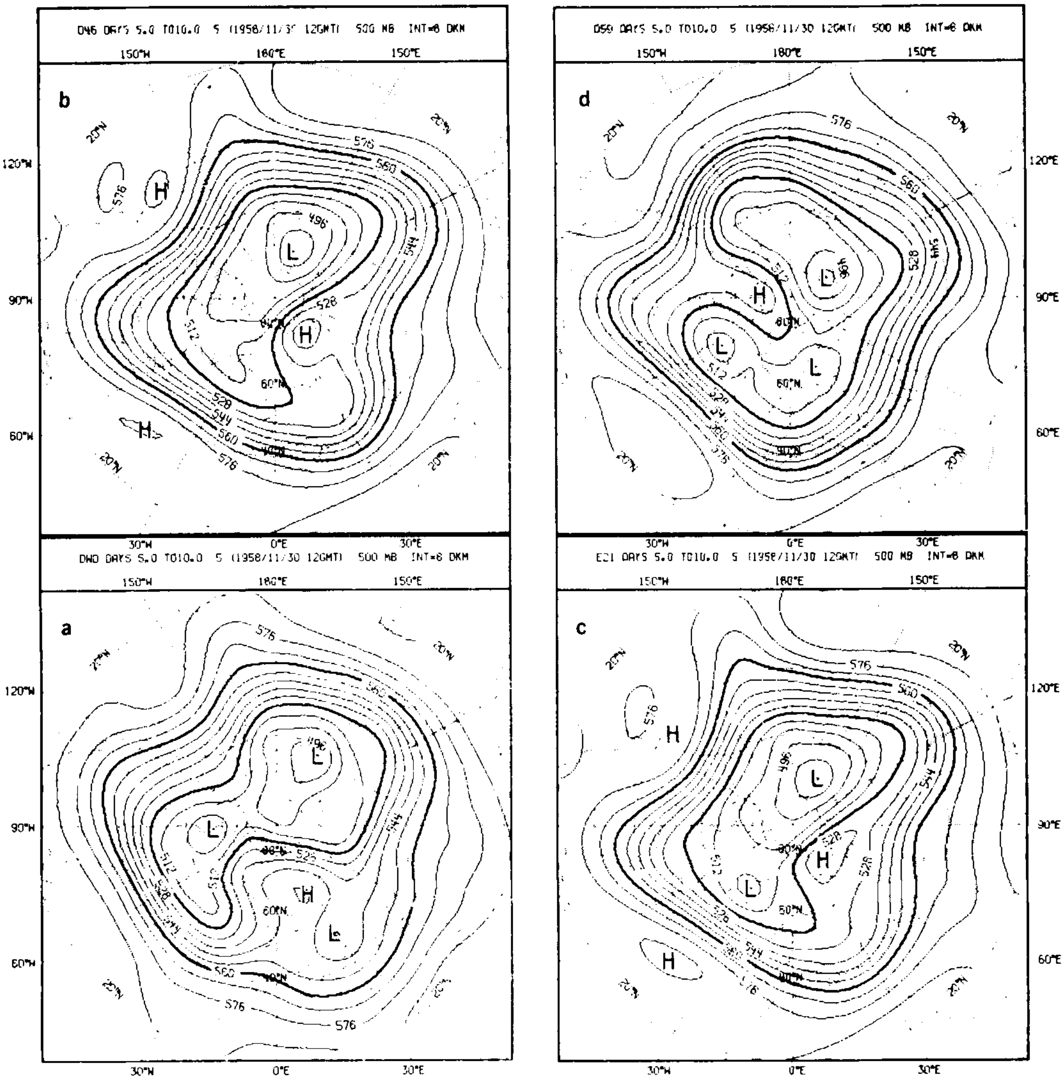

Fig. 15. As Fig. 14, but for 500 mb geopotential height and for days 5 to 10. Contours are drawn every 8 dam.

E21, some consideration can be given to the rôle of the Alps on European meteorology. Fig. 16a shows 5-day mean difference maps E21–D46 averaged over the first half of the experiments (day 0 to day 5), the lower part showing 1000 mb height and the upper 500 mb height. Fig. 16b shows the same, but for day 2 only. These maps illustrate the character of the disturbance produced by the enhanced model Alps: it has a dipole structure confined near the mountain, but with a horizontal scale much larger than the mountain itself. Besides the low centre south of the Alps, a high centre of comparable amplitude is evident to the north (or north east). By examining the daily sequence of instantaneous difference fields (only day 2 shown here, see Fig. 16b), one can estimate the growth rate of this disturbance, which has a doubling time of about 15 h in the first 2 days. A tendency of propagation downstream (towards the north-east) can also be observed, in accordance with the Rossby wave propagation in the lee of mountains as described in Grose and Hoskins (1979). The lee cyclogenesis

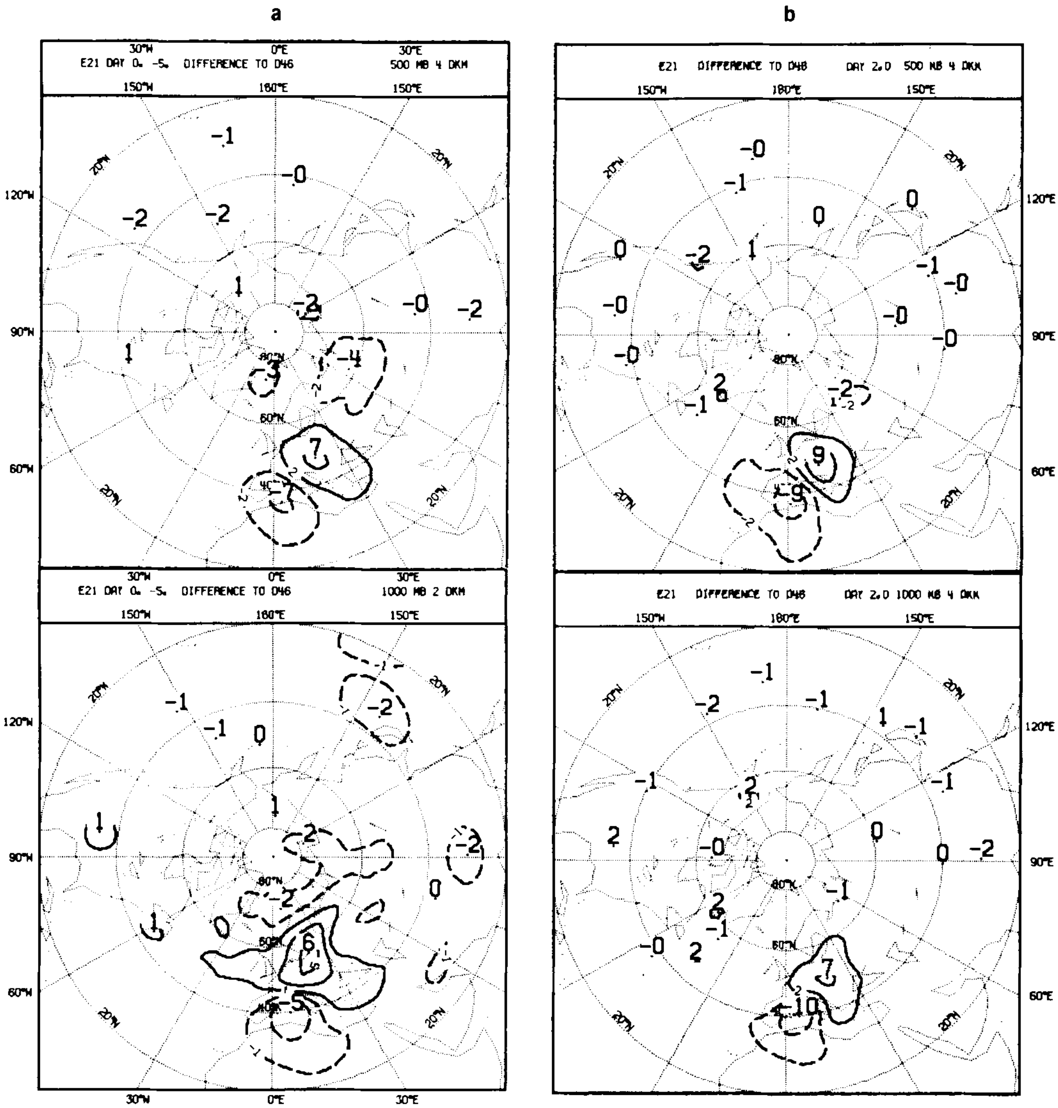

Fig. 16. (a) Days 0 to 5 mean difference map between experiment E21 (enhanced Alps) and experiment D46 (control). Top: 500 mb geopotential height-lines every 4 dam. Bottom: 1000 mb geopotential height-lines every 2 dam. (b) As (a) but for day 2 only. Lines every 4 dam top and bottom.

phenomena is not, therefore, only a meso-scale process confined to the immediate lee of the Alps, but is part of a structured disturbance that affects the whole European region.

A comparison between Figs. 16a and b also highlights another important feature of the influence of the Alps. While at day 2 the disturbance shows no appreciable tilt with height, the 5-day mean map shows a low-level doublet oriented NE–SW and an upper-level disturbance oriented almost N–S. This indicates that while the linear orographic perturbation is essentially equivalent-barotropic, the interaction of such a forcing with a baroclinic "basic state" atmospheric flow develops structures (lee-cyclones) able to grow at the expense of the available potential energy of such a basic state and is therefore baroclinic in nature. This supports the conclusions of Tibaldi et al. (1980) with results of a global model, not contaminated, therefore, by spurious lateral boundary conditions typical of limited area and channel models.

6. Conclusions

In summary, the following conclusions can be drawn from the experiments.

(i) It is confirmed that the Alps are responsible for the case of Mediterranean cyclogenesis under consideration, and participate in the control of its evolution with time.

(ii) This cyclogenetic effect is not simulated if the orography is "smoothed" in the model, as in the first version used.

(iii) The same effect is, instead, obtained by simply increasing the height of the Alps to a realistic value that produces a blocking effect on the oncoming flow.

(iv) The difference fields between experiments with and without the Alps reveal that the mountain-induced perturbation, although initially barotropic, develops baroclinically in time. This perturbation is characterized not only by a depression-inducing field in the south-south-west of the barrier but also by a positive geopotential anomaly centre to the north-east of it. The horizontal extent of this induced perturbation is on the European Scale.

(v) Concerning the specific relationship between cyclogenesis in the lee of the Alps and blocking that originally prompted this investigation, these experiments cannot be taken as conclusive, chiefly for the reason that none of them predict the onset of the blocking situation which follows the cyclogenesis with an accuracy sufficient to make them sensitive to the evolution of the previous synoptic development. More work is therefore needed to investigate this aspect.

(vi) The importance of planetary orography as a principal source of quasi-stationary ultra-long waves is shown as well as the rôle of such waves in maintaining atmospheric blocking.

7 Acknowledgements

The authors are indebted to A. Speranza for numerous discussions that led to the formulation of this numerical experiment. The calculations were carried out on the ECMWF computer system using resources of the ECMWF Research Department and of the Italian Weather Service (Servizio Meteorologico dell'Aeronautica Militare). We gratefully acknowledge their support.

REFERENCES

Arakawa, A. 1966. Computational design for long-term numerical integration of the equations of fluid motion: two-dimensional incompressible flow. Part 1. *J. Comp. Phys. 1*, 119–143.

Arakawa, A. and Lamb, V. R. 1977. Computational design of the basic dynamical processes of the UCLA general circulation model. *Methods in Computational Physics*, vol. 17 (Ed. J. Chang). Academic Press.

Austin, J. F. 1980. The blocking of mid-latitude westerly winds by planetary waves. *Q. J. R. Meteorol. Soc. 106*, 327–350.

Bengtsson, L. 1981. Numerical prediction of atmospheric blocking—a case study. *Tellus 33*, 19–42.

Berggren, R., Bolin, B. and Rossby, C. G. 1949. An aerological study of zonal motion, its perturbations and break-down. *Tellus 1*, 14–37.

Berkofsky, L. and Bertoni E. A. 1955. Mean topographic charts for the entire earth. *Bull. Am. Meteorol. Soc. 36*, 350–354.

Bleck, R. 1977. Numerical simulation of lee cyclogenesis in the Gulf of Genoa. *Mon. Wea. Rev. 105*, 428–445.

Burridge, D. M. 1979. Some aspects of large-scale numerical modelling of the atmosphere. *Proceedings of ECMWF Seminar on Dynamical Meteorology and Numerical Weather Prediction*, vol. 2, 1–78.

Burridge, D. M. and Haseler, J. 1977. A model for medium-range weather forecasting—a diabatic formulation. *ECMWF Tech. Rep. No. 4*.

Buzzi, A. and Tibaldi, S. 1978. Cyclogenesis in the lee of the Alps: a case study. *Q. J. R. Meteorol. Soc. 104*, 271–287.

Charney, J. G. and Eliassen, A. 1949. A numerical method for predicting the perturbations of the middle latitude westerlies. *Tellus 1*, 38–54.

Charney, J. G. and De Vore, J. G. 1979. Multiple flow equilibria in the atmosphere and blocking. *J. Atmos. Sci. 36*, 1205–1216.

Charney, J. G. and Straus, D. M. 1980. Form-drag instability, multiple equilibria and propagating planetry waves in baroclinic, orographically forced, planetary wave systems. *J. Atmos. Sci. 37*, 1157–1176.

Colucci, S. J., Loesh, A. Z. and Bosart, L. F. 1981. Spectral evolution of a blocking episode and comparison with wave interaction theory. *J. Atmos. Sci. 38*, 2092–2111.

Green, J. S. A. 1977. The weather during July 1976: some dynamical considerations on the drought. *Weather 32*, 120–126.

Grose, W. L. and Hoskins, B. J. 1979. On the influence of orography on large-scale atmospheric flow. *J. Atmos. Sci. 36*, 223–234.

Hartmann, D. L. and Ghan, S. J. 1980. A statistical study of the dynamics of blocking. *Mon. Wea. Rev. 108*, 1144–1159.

Hollingsworth, A., Arpe, K. Tiedtke, M. Capaldo, M. and Savijärvi, H. 1980. The performance of a medium-range forecast model in winter—impact of physical parameterizations. *Mon. Wea. Rev. 108*, 1736–1773.

Illari, L. Malguzzi, P. and Speranza, A. 1981. On breakdowns of the Westerlies. *Geophys. Astrophys. Fluid Dyn. 17*, 27–49.

Ji, L. R. and Tibaldi, S. 1982. Numerical simulations of a case of blocking: the effects of orography and land-sea contrast. *ECMWF Tech. Rep. No. 33.*

Malguzzi, P. and Speranza, A. 1981. Local multiple equilibria and regional atmospheric blocking. *J. Atmos. Sci. 38*, 1939–1948.

Manabe, S. and Terpstra, T. B. 1974. The effects of mountains on the general circulation of the atmosphere as identified by numerical experiments. *J. Atmos. Sci.* **31**, 3–42.

McWilliams, J. C. 1980. An application of equivalent modons to atmospheric blocking. *Dyn. Atmos. Oceans 5*, 43–66.

Phillips, N. A. 1957. A coordinate system having some special advantages for numerical forecasting. *J. Meteorol. 14*, 184–185.

Rex, D. F. 1950. Blocking action in the middle troposphere and its effect upon regional climate. *Tellus 2*, 196–211 and 275–301.

Sadourny, R. 1975. The dynamics of finite difference models of the shallow-water equations. *J. Atmos. Sci. 32*, 680–689.

Temperton, C. and Williamson, D. L. 1981. Normal mode initialization for a multi-level grid-point model. Part I: linear aspects. *Mon. Wea. Rev. 109*, 729–743.

Tibaldi, S. 1980. Cyclogenesis in the lee of orography and its numerical modelling, with special reference to the Alps, in *Orographic effects in planetary flows* (eds. R. Hide and P. White). GARP Publ. Series No. 23, Chapter 7, pp. 207–232. Geneva: WMO.

Tibaldi, S. and Ji, L. R. 1983. On the effect of model resolution on numerical simulation of blocking. *Tellus 35A*, 28–38.

Tibaldi, S. and Buzzi, A. 1982. Orographic influences on Mediterranean lee cyclogenesis and European blocking in a global numerical model. *ECMWF Tech. Rep. No. 29.*

Tibaldi, S., Buzzi, A. and Malguzzi, P. 1980. Orographically-induced cyclogenesis: analysis of numerical experiments. *Mon. Wea. Rev. 108*, 1302–1314.

Tiedtke, M., Geleyn, J-F. Hollingsworth, A. and Louis, J-F. 1979. ECMWF model-parameterization of sub-grid scale processes. *ECMWF Tech. Rep. No. 10.*

Trevisan, A. and Buzzi, 1980. Stationary response of barotropic weakly non-linear Rossby waves to quasi-resonant orographic forcing. *J. Atmos. Sci. 37*, 947–957.

Williamson, D. L. and Temperton, C. 1981. Normal-mode initialization for a multilevel grid-point model. Part II: Non-linear aspects. *Mon. Wea. Rev. 109*, 744–751.